vol. 170, no. 4 the american naturalist october 2007

E-Article

Species Associations in a Heterogeneous Sri Lankan Dipterocarp Forest

Thorsten Wiegand,[1,*] Savithri Gunatilleke,[2,†] and Nimal Gunatilleke[2,†]

1. UFZ Helmholtz Centre for Environmental Research–UFZ, Department of Ecological Modeling, PF 500136, D-04301 Leipzig, Germany;
2. University of Peradeniya, Faculty of Science, Department of Botany, Peradeniya 20400, Sri Lanka

Submitted January 15, 2007; Accepted June 14, 2007; Electronically published August 15, 2007

abstract: We used point pattern analysis to examine the spatial distribution of 46 common tree species (diameter at breast height >10 cm) in a fully mapped 500 × 500-m tropical forest plot in Sinharaja, Sri Lanka. We aimed to disentangle the effect of species interactions (second-order effects) and environment (first-order effects) on the species' spatial distributions. To characterize first-order associations (segregation, overlap), we developed a classification scheme based on Ripley's K and nearest-neighbor statistics. We subsequently used heterogeneous Poisson null models, accounting for possible environmental heterogeneity, to reveal significant uni- and bivariate second-order interactions (regularity, aggregation and repulsion, attraction). First-order effects were strong; overall, 53% of all species pairs occupied largely disjoint areas (segregation), 40% showed partial overlap, and 6% overlapped. Only 5% of all species pairs showed significant second-order effects, but about half of the species showed significant intraspecific effects. Significant plant-plant interactions occurred mostly within 2–4 m and disappeared within 15–20 m of the focal plant. While lack of significant species interactions suggests support for the unified neutral theory, species' observed spatial segregation does not support the assumptions of the neutral theory. The strong observed tendency of species to segregate may have supplementary effects on other processes promoting species coexistence.

Keywords: coexistence, habitat association, pair-correlation function, plant-plant interactions, point pattern analysis, tropical forest.

* E-mail: thorsten.wiegand@ufz.de.

† E-mail: savnim@slt.lk.

Am. Nat. 2007. Vol. 170, pp. E77–E95.
0003-0147/2007/17004-42335$15.00.
DOI: 10.1086/521240

A persistent challenge in ecology is to explain the high species diversity of tropical forests (Chesson 2000; Wright 2002). It is still poorly understood which processes govern the composition and assembly in species-rich communities. Several competing hypotheses have been developed and tested but lead to contrasting results (Janzen 1970; Connell 1978; Hubbell et al. 1999; Chave et al. 2002; Volkov et al. 2005). Recently, neutral theory (Hubbell 2001; Chave 2004) has caused a heated debate around the determinants of diversity and species composition in species-rich communities (e.g., Clark and McLachlan 2003; McGill 2003; Tilman 2004; Hubbell 2005; Wootton 2005; Condit et al. 2006; Wills et al. 2006). The assumption that species may be functionally identical and drift randomly in abundance until they vanish "contradicts almost everything that ecologists have to come to understand about species diversity and its maintenance in communities" (Missa 2005, p. 13) and suggests that many mechanisms that have long been studied are unimportant for certain community attributes.

However, there is ample evidence that species are not equivalent but that species-specific differences in their traits and ecological strategies affect population dynamics and the functioning of the entire community. Plant species can have strong direct and indirect positive and negative effects on other species (Hubbell et al. 2001; Peters 2003; Lortie et al. 2004; Uriarte et al. 2004; Stoll and Newbery 2005), and niche theory outlines that species differ in several trade-offs, such as high-light growth rate versus low-light survival (Bazzaz 1996; Pacala et al. 1996), competition versus colonization (Levins and Culver 1971), seed size versus seed number (Dalling and Hubbell 2002), differential segregation along environmental gradients (Harms et al. 2001; Valencia et al. 2004; Gunatilleke et al. 2006), and different resistance to pests (Wright 2002; Peters 2003).

Several of the processes that have been hypothesized for explaining species coexistence and community structure have a strong spatial component. Examples include direct plant-plant interactions, such as competition or facilitation (Callaway and Walker 1997; Bruno et al. 2003; Lortie et al. 2004), dispersal limitation (Wong and Whitmore 1970;

Hubbell 1997, 2001), habitat preference (Harms et al. 2001; Gunatilleke et al. 2006), and the Janzen-Connell hypothesis (Janzen 1970; Connell 1971). Hubbell et al. (2001, p. 860) summarized the original premise for creating and monitoring the large Barro Colorado Island (BCI), Panama, forest dynamics plot (FDP): "Whatever coexistence mechanisms were operating in the BCI forest, they should leave a spatial signature that could be detected by making explicit maps of individual tree locations in the BCI forest." Data provided by the network of large permanent FDPs, coordinated by the Center for Tropical Forest Science (CTFS), now allow the investigation as to whether there are detectable spatial signatures of the mechanisms that regulate tree species diversity. At these plots, all stems >1 cm diameter at breast height (DBH) are identified, measured, mapped, and monitored (Condit 1998). In this article, we analyze data from the FDP at Sinharaja, Sri Lanka, to investigate whether, and at what spatial scales, positive or negative species-species associations occur and whether they are significant.

Methods for the spatial analysis of point patterns, that is, data sets consisting of mapped locations of plants as provided by the FDP plots, are well established (Ripley 1981; Stoyan and Stoyan 1994; Dale 1999; Diggle 2003; Møller and Waagepetersen 2003) and allow the assessment of the spatial association of pairs of species occurring at a given study area. Especially useful are second-order statistics such as the pair-correlation function or Ripley's K, which are based on the distribution of distances of pairs of points (Ripley 1981) and describe the characteristics of point patterns over a range of distances. This is an important property because it reveals critical scales below which significant associations occur and at which scales they becomes positive, negative, or neutral. Null models are of particular importance in this context because they represent the null hypothesis about the point pattern that is contrasted with the observed data (Diggle 2003; Schurr et al. 2004; Wiegand and Moloney 2004). Null models allow one to determine whether a hypothesized effect is significant and at what scale. A practical approach to assess significant departure from the null hypothesis is to run Monte Carlo simulations of a point process corresponding to the null hypothesis and to construct simulation envelopes of an appropriate test statistic (Stoyan and Stoyan 1994; Diggle 2003).

However, studying species-species association is not always straightforward because first-order effects (i.e., habitat preference, where the occurrence of the species at the plot depends on altitude, shading, soil moisture, nutrients, etc.) may confound second-order effects (i.e., direct plant-plant interactions, such as competition or facilitation within or among species). Separation of first- and second-order effects is also an important biological issue because habitat preference and plant-plant interactions represent different hypotheses for explaining species coexistence and community structure. Specific methods are required to carefully separate both effects (e.g., Baddeley et al. 2000; Diggle 2003). Here we use an approach based on separation of scales. Several studies using individual-based analyses of local neighborhood effects on growth and survival showed that direct plant-plant interactions may operate only in local plant neighborhoods (within <20 or 30 m), fading away at larger scales (Hubbell et al. 2001; Uriarte et al. 2004). For example, Hubbell et al. (2001) found that the neighborhood effects of conspecific density disappear within approximately 12–15 m of the focal plant, and Uriarte et al. (2004) found in a study on sapling growth that growth of target species responded only to neighbors within a distance <20 m. On the other hand, habitat conditions for trees, that is, elevation, orientation, and soil nutrients, vary typically at larger scales along environmental gradients that are often related to topographical features such as slope and elevation (Harms et al. 2001; Diggle 2003; Valencia et al. 2004; Gunatilleke et al. 2006; John et al. 2007). This suggests use of heterogeneous Poisson processes (Stoyan and Stoyan 1994; Wiegand and Moloney 2004) as null models that retain the large-scale structure of the pattern but remove its small-scale correlation structure.

In this article, we study all species-species associations occurring between 46 frequent species at the fully censused 25-ha FDP at Sinharaja, Sri Lanka. We first develop a method to roughly categorize the first-order association of heterogeneous bivariate patterns and apply it to the resulting 2,070 species pairs. Next we use point pattern analysis in combination with heterogeneous Poisson null models to identify species and species pairs with significant second-order effects. Finally, we investigate whether significant effects were correlated with the degree of univariate clustering and species abundances.

Methods

Study Site and Study Species

The area studied is the 25-ha Sinharaja FDP, a 500 × 500-m permanent study plot that is located in the lowland rain forest of the Sinharaja UNESCO World Heritage Site at the center of the ever-wet southwestern region of Sri Lanka, at 6°21′–26′N and 80°21′–34′E. The Sinharaja FDP is representative of the ridge–steep slope–valley landscape of the lowland and midelevational rain forests of southwestern Sri Lanka. The forest has been classified as a *Mesua-Doona* community (de Rosayro 1942), and on a regional scale, it represents a mixed dipterocarp forest (Ashton 1964; Whitmore 1984). The floristic ecology and

forest structure within the plot as a whole have been documented by Gunatilleke et al. (2004). Topographically, the Sinharaja FDP spans an elevational range of 151 m, rising from 424 to 575 m above sea level. The Sinharaja FDP includes a central valley at about 430 m lying between two slopes; a steeper, higher slope facing the southwest; and a less steep slope facing the northeast. Tree species show varying degrees of associations to habitat types defined through elevation, slope, and convexity (Gunatilleke et al. 2006).

Vegetation Sampling

The established methodology of Hubbell and Foster (1983) and Manokaran et al. (1992) was followed to maintain uniformity in the establishment and sampling of similar plots within the CTFS network. The Sinharaja FDP was established in 1993, when it was demarcated on the horizontal plane into 625 20 × 20-m (400 m^2) plots. The trees in the plot were censused over the period 1994–1996, when the diameters of all freestanding stems >1 cm DBH were measured. Each stem was mapped and identified as to species using the National Herbarium of Sri Lanka and Dassanayake and Fosberg (1980–2000).

We analyzed the spatial pattern of nonjuvenile trees with DBH >10 cm. To obtain a sufficiently large sample size for the point pattern analyses, we used only 46 species with more than 70 nonjuvenile trees.

Spatial Pattern Analysis

We used univariate and bivariate pair-correlation functions to analyze the spatial pattern of individual species and the association of the patterns of two tree species at different spatial scales r (Stoyan and Stoyan 1994). The pair-correlation function is closely related to Ripley's K function (Ripley 1976); both are based on the distribution of distances of all pairs of points of the patterns. The bivariate K function $K_{12}(r)$ can be defined as the expected number of pattern 2 points within distance r of an arbitrary pattern 1 point, divided by the intensity λ_2 of pattern 2 (Ripley 1976). The bivariate pair-correlation function $g_{12}(r)$ is related to the derivative of the K function; that is, $g_{12}(r) = K'_{12}(r)/(2\pi r)$ (Ripley 1977; Stoyan and Stoyan 1994). Analogously, the univariate K function is the expected number points within distance r of an arbitrary point divided by the intensity of points, but the focal points are not counted. Further details can be found in standard textbooks (e.g., Ripley 1981; Stoyan and Stoyan 1994; Diggle 2003).

An important difference between K and g functions is that the K function is accumulative; that is, it counts pattern 2 points within entire circles centered on pattern 1 points, whereas the pair-correlation function is nonaccumulative and uses only points separated by a certain distance r. Therefore, if a departure from a null model occurred, the assessment of scales of significant point-point interactions is difficult with the K function because the values of K at small scales compromise the values of K at larger scales (Wiegand and Moloney 2004; Loosmore and Ford 2006). The pair-correlation function, in contrast, allows for a precise assessment of scales where significant point-point interactions occur. All analyses were done with the grid-based software Programita (Wiegand and Moloney 2004). Note that the spatial resolution of the grid should be larger than the measurement error but fine enough to capture the scales of interest with sufficient resolution.

Classification Scheme of Large-Scale First-Order Association

The tree species at the Sinharaja FDP are characterized by a high degree of habitat association (Gunatilleke et al. 2006), which suggests that most species may show heterogeneous spatial patterns. First-order effects due to habitat association may mediate positive association if both species prefer the same type of habitat (mixing or overlap) and negative association (segregation) if they prefer different types of habitat. As a first step of our analysis, we developed a simple scheme to classify first-order association of bivariate heterogeneous patterns. We applied this scheme for describing the relative frequency of each association type at our study site. The classification scheme can also be used to compare different FDP plots and is of interest for general theory of species coexistence in species-rich communities.

The two axes of our scheme are spanned by two measures commonly used in point pattern analysis, the bivariate K function $K_{12}(r)$ and the bivariate emptiness probability $P_0(r)$ (i.e., the probability that a circle with radius r centered in a pattern 1 point contains no pattern 2 point; Diggle 2003). Note that the K function and the emptiness probability evaluate two fundamentally different aspects of bivariate point patterns. The quantity $\lambda_2 K_{12}(r)$ is the expected number of pattern 2 points within distance r of an arbitrary pattern 1 point. However, $\lambda_2 K_{12}(r)$ alone does not unambiguously characterize heterogeneous patterns because the same expectation for $\lambda_2 K_{12}(r)$ may arise if (1) many pattern 1 points have no pattern 2 neighbor but few pattern 1 points have many pattern 2 neighbors or (2) all pattern 1 points have a similar number of pattern 2 neighbors. The bivariate emptiness probability $P_0(r)$, which evaluates only the nearest pattern 2 points within distance r of pattern 1 points, however, is able to differentiate between situations: it will have high values if many pattern 1 points have no pattern 2 neighbor and low values if the

pattern 1 points all have a similar number of pattern 2 neighbors. The $P_0(r)$ thus provides additional information not provided by $\lambda_2 K_{12}(r)$.

To define the two axes we first needed to specify an appropriate spatial scale r_L to calculate $K_{12}(r_L)$ and $P_0(r_L)$. We used a spatial scale r_L that was slightly larger than the typical range of plant-plant interactions in tropical forests (i.e., $r_L = 30$ m; e.g., Hubbell et al. 2001; Uriarte et al. 2004). We normalized the axes by subtracting the theoretical values for homogeneous patterns without second-order effects (i.e., $K^h(r_L) = \pi r_L^2$ and $P_0^h(r_L) = \exp(-\lambda_2 \pi r_L^2)$; see appendix). The two axes P and M are thus defined as

$$P = -\hat{P}_0(r_L) + \exp(-\lambda_2 \pi r_L^2),$$

$$M = \ln(\hat{K}_{12}(r_L)) - \ln(\pi r_L^2). \quad (1)$$

We log transformed the K function to weight departures in both directions equally and scaled P and M to yield positive values if there were more pattern 2 points than expected (K function) or if the probability of having a nearest pattern 2 neighbor within distance r_L was greater than expected (emptiness probability). Note that the P axis ranges theoretically between -1 and 0.45 (see appendix). The M axis may theoretically reach $M = -\infty$ for complete segregation and may have large values if the two patterns occupy the same small subarea.

Our scheme allows four different types of bivariate associations. The two patterns are segregated for $P < 0$ and $M < 0$ (type I; fig. 1*A*). First, there are on average fewer points of pattern 2 within neighborhoods (with radius r_L) around points of pattern 1 than expected without first- and second-order effects (i.e., $M < 0$). Second, the probability that a point of pattern 1 has its nearest point of pattern 2 within distance r_L is smaller than expected (i.e., $P < 0$). For $P < 0$ and $M > 0$, the association is characterized by partial overlap (type II; fig. 1*B*), where many points of pattern 1 have no pattern 2 neighbors within distance r_L (i.e., $P < 0$), but the overlap of both patterns is large enough to make M positive. For $P > 0$ and $M > 0$, the two patterns occur within the same area (mixing; type III; fig. 1*C*). Additionally, there is a fourth type ($P > 0$, $M < 0$), which can occur only if second-order effects are strong (see appendix). We derived analytical approximations of the K function and the emptiness probability for simple cases of heterogeneity (see appendix) to explore the properties of our scheme in more detail and to assure that it behaved in the expected way.

Null Models

To identify significant species-species associations occurring at the Sinharaja FDP, we proceeded in three steps. We first analyzed second-order effects in the univariate patterns (analysis 1), next we analyzed second-order effects in the bivariate patterns (analysis 2), and finally we tested for significant large-scale association to find out how frequently species pairs share the same subareas of the FDP (analysis 3). In all cases, we used heterogeneous Poisson null models to account for possible first-order effects.

Heterogeneous Poisson Point Processes

First- and second-order effects may interact (Wiegand and Moloney 2004). The most exact approach to reveal significant second-order effects would involve development of habitat models, that is, building statistical models to predict the probability of occurrence of a tree of a given species in space as a function of environmental covariates (Guisan and Thuiller 2005) and then using inhomogeneous K or g functions (Baddeley et al. 2000) to investigate second-order effects (e.g., Diggle et al. 2007). However, this becomes a very tedious task when there are high numbers of species and maps of environmental covariates are

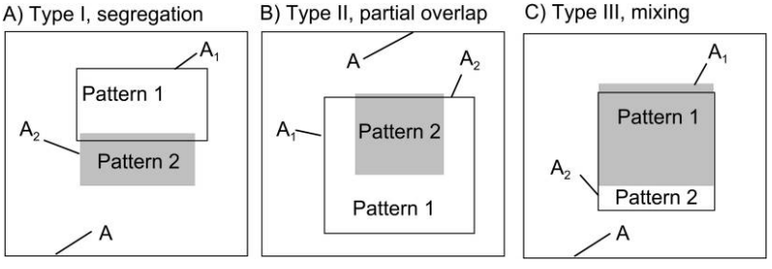

Figure 1: Schematic representation of the three most important types of association between two heterogeneous patterns. Pattern 1 occupies subarea A_1 (*white*) and pattern 2 subarea A_2 (*gray*) of study area A. The three cases arise through different degree of overlap between A_1 and A_2. *A*, Segregation: there is little or no overlap between A_1 and A_2. *B*, Partial overlap: the points of pattern 2 are located mostly within A_1, but there are many pattern 1 points that have no pattern 2 neighbors within distance r_L. *C*, Mixing: A_1 and A_2 overlap to a large degree.

not readily available with a fine spatial resolution. A shortcut based on separation of scales is to use heterogeneous Poisson point processes where small-scale effects are attributed to second-order plant-plant interactions and large-scale effects are attributed to environmental heterogeneity (Diggle 2003). In heterogeneous Poisson point processes, the occurrence of any point is independent of that of any other, but the points are distributed in accordance with an intensity function $\lambda(x, y)$ that varies with location (x, y) (Stoyan and Stoyan 1994; Wiegand and Moloney 2004).

We used an Epanečnikov kernel, a nonparametric method recommended by Stoyan and Stoyan (1994), to estimate the intensity function of a given point pattern. The Epanečnikov kernel is defined as

$$e_h(d) = \begin{cases} \frac{3}{4h}\left(1 - \frac{d^2}{h^2}\right) & -h \le d \le h \\ 0 & \text{otherwise} \end{cases}, \qquad (2)$$

where d is the distance from a focal point and h is the bandwidth. For a given location (x, y), the intensity $\lambda(x, y)$ is constructed by using a moving window with circular shape and radius h around location (x, y) and summing all points in the circle but weighting them with factor $e_h(d)$ according to their distance d from the focal location (x, y). Clearly, the intensity estimate depends on the bandwidth h: for large h, one obtains smooth intensity functions, and for small h, the estimated function is rough and may obscure the fundamental structure of the distribution (Stoyan and Stoyan 1994). We used a biological argument and defined the bandwidth h as the maximal scale at which second-order effects are expected in tropical forests.

Analysis 1: Univariate Plant-Plant Interactions

To reveal significant second-order effects in the univariate patterns (i.e., regularity and aggregation), we constructed the intensity function $\lambda(x, y)$ based on the pattern of the species under study and selected for all 46 species a bandwidth $h = 30$ m. This scale is slightly larger than typical scales at which local point-point interactions have been analyzed in tropical forests (e.g., Hubbell et al. 2001; Peters 2003; Uriarte et al. 2004; Stoll and Newbery 2005), but it is smaller than the range over which the environmental gradients may vary (e.g., Harms et al. 2001; Valencia et al. 2004; Gunatilleke et al. 2006; John et al. 2007). We studied plant-plant interactions with a spatial resolution of 2 m up to 40 m. This is a sufficiently fine resolution to capture detailed variation in the pair-correlation function over the rage of scales where we expected significant effects (i.e., up to some 30 m), but it is coarse enough to yield feasible computation time for the high number of point pattern analyses required.

Analysis 2: Bivariate Plant-Plant Interactions

To reveal significant second-order effects in the bivariate patterns (i.e., repulsion and attraction), we kept the location of the trees of the first species fixed and randomized the locations of the trees of the second species using a heterogeneous Poisson null model. Here the intensity function $\lambda_2(x, y)$ was constructed based on pattern 2. Again, we used a bandwidth $h = 30$ m and a spatial resolution of 2 m. This null model allowed us to assess whether pattern 2 points were more or less frequently around pattern 1 points than expected by the intensity of pattern 2, which would indicate attraction or repulsion, respectively. Note that we tested all pairs, that is, species 1 versus species 2 and species 2 versus species 1, since we cannot assume that the interaction will be symmetric.

Analysis 3: Large-Scale Species-Species Associations

Most species in tropical forests are clustered at some spatial scale (e.g., Condit et al. 2000). This is particularly true at the Sinharaja plot, where 80% of 125 species studied showed significant habitat association (Gunatilleke et al. 2006). An interesting question is therefore how often two species share the same areas, that is, how often they show positive association at scales above the typical scale where plant-plant interactions occur. To answer this question, we used the null hypothesis that species 2 followed the intensity of species 1. The corresponding null model was again a heterogeneous Poisson null model where the locations of the trees of species 1 were fixed, but the locations of the trees of the second species were randomized in accordance with the intensity of species 1. In this analysis, we used a bandwidth of $h = 50$ m to estimate the intensity of species 1 and a spatial resolution of 5 m because we were interested only in larger-scale effects. In the appendix, we show that this null model is met (for patterns without second-order effects) if the area occupied by species 2 is contained within the area occupied by species 1 (e.g., fig. 1*B*). Thus, we expect that bivariate patterns that meet the null model may show partial overlap (type II) or mixing (type III).

Monte Carlo Simulations

For all analyses, we performed 99 Monte Carlo simulations of the null model and used the fifth-lowest and fifth-highest simulated $g(r)$ values as simulation envelopes. The 99 simulations generated sufficiently smooth simulation envelopes and were sufficient for our purpose given the high

number of analyses required. Significant departure from the null model occurred at scale r if the empirical pair-correlation function was outside the simulation envelopes. However, because of simultaneous inference (i.e., we tested at several spatial scales r simultaneously), Type I error may occur if the value of $g(r)$ is close to a simulation envelope (i.e., the null model may be rejected even if it is true; Loosmore and Ford 2006). We therefore combined the common simulation envelope method with a goodness-of-fit test (Diggle 2003).

In short, the goodness-of-fit (GOF) test collapses the scale-dependent information contained in the pair-correlation function into a single test statistic u_i that represents the total squared deviation between the observed pattern and the theoretical result across the distances of interest. The u_i values were calculated for the observed data ($i = 0$) and for the data created by the $i = 1, \ldots s$ simulations of the null model, and the rank of u_0 among all u_i is determined. The observed p value of this test is

$$\hat{p} = 1 - \frac{\sum_{j=1}^{s} I(u_0 > u_j)}{s + 1}, \tag{3}$$

where $I(u_0 > u_j)$ is an indicator function that equals 1 if $u_0 > u_j$ and equals 0 otherwise (Loosmore and Ford 2006). Details can be found in work by Diggle (2003) and Loosmore and Ford (2006).

Depending on our biological question, we selected distance intervals of 0–20 m (analyses 1 and 2) and 50–250 m (analysis 3) to assess departures from the null model for application of the GOF test. We then retained data sets for further analysis only where the observed p value of the hypothesis test was smaller than .05 (analyses 1 and 2) or larger than .05 (analysis 3). Note that analysis 3 assumes a specific association, and by considering only data sets with observed p values larger than .05, we selected the cases where the null model was met, that is, indicating significant large-scale association.

Results

Classification Scheme of Bivariate Associations

Figure 2*A* shows how the 2,070 species pairs were allocated within the two-dimensional classification space. The large-scale associations were not equally distributed among types. The two most frequent associations were segregation (type I; fig. 2*E*), which occurred in 53.2% of all cases, and partial overlap (type II; fig. 2*B*), which occurred in 40.3% of all cases. However, mixing (type III; fig. 2*C*) occurred in only 6.1% of all cases. As expected, type IV association occurred in only 0.4% of all cases (fig. 2*E*). Notably, 12.2% of all species-species pairs showed strong segregation on both classification axes (i.e., $P < -0.5$, $M < -1$; fig. 2*E*). Note that the results for a number of species pairs are not mutually independent; we tested the pair A-B as well as B-A, and testing the pair A-C is not independent of tests of A-B and B-C.

Analysis 1: Univariate Plant-Plant Interactions

The 46 species showed diverse spatial patterns (fig. 3). None of the species showed a univariate pair-correlation function with significant regularity at scales $r \geq 2$ m, but all species showed significant aggregation when confronted with a homogeneous Poisson null model (results not shown). For 24 of the 46 species, the GOF test revealed a significant departure from the heterogeneous Poisson null model (at scales 0–20 m). Twenty-one species showed small-scale aggregation (fig. 3*B*, 3*D*, 3*F*), the two species *Myristica dactyloides* (fig. 3*J*) and *Xylopia championii* (fig. 3*L*) showed significant regularity at scale $r = 0$ m (i.e., points within the same grid cell), and the other 22 species followed the heterogeneous Poisson null model.

Figure 3 also illustrates the strong influence of topography on the spatial distribution of the tree species at Sinharaja (Gunatilleke et al. 2006). One important habitat type is given by upper-elevation habitats such as steep spurs where, for example, the species *Mesua nagassarium* (fig. 3*E*) is found, and upper steep and less steep gullies where, for example, the species *Mesua ferrea* is found. On the other hand, the species *Schumacheria castaneifolia* (fig. 3*C*) and *Chaetoarpus castanocarpus* (fig. 3*G*) are found in the lower-elevation habitats.

To obtain a rough estimate of the magnitude of scale-dependent effects of regularity and aggregation, we counted for each scale r the number of species (using only species where the rank of the GOF test was >95) for which the pair-correlation function was above or below the fifth-highest or fifth-lowest value of the pair-correlation function in the 99 Monte Carlo simulations. The frequency of aggregation peaked at scales between 0 and 8 m and was almost 0 at scales $r > 16$ m (fig. 4*A*). Interestingly, the heterogeneous Poisson null model that removed all non-random spatial structures below 30 m (by randomizing the pattern using its intensity) led us to expect that significant effects may occur at scales <30 m. However, we found that significant effects already disappeared at 16 m. This suggests a clear separation of scales where univariate plant-plant interactions occur predominantly at scales shorter than 16 m and other effects due to habitat association at scales larger than 30 m. This result also justifies our approach of separation of scales to reveal second-order effects. In contrast, if significant effects disappear only at scales of about 30 m (i.e., the bandwidth of the hetero-

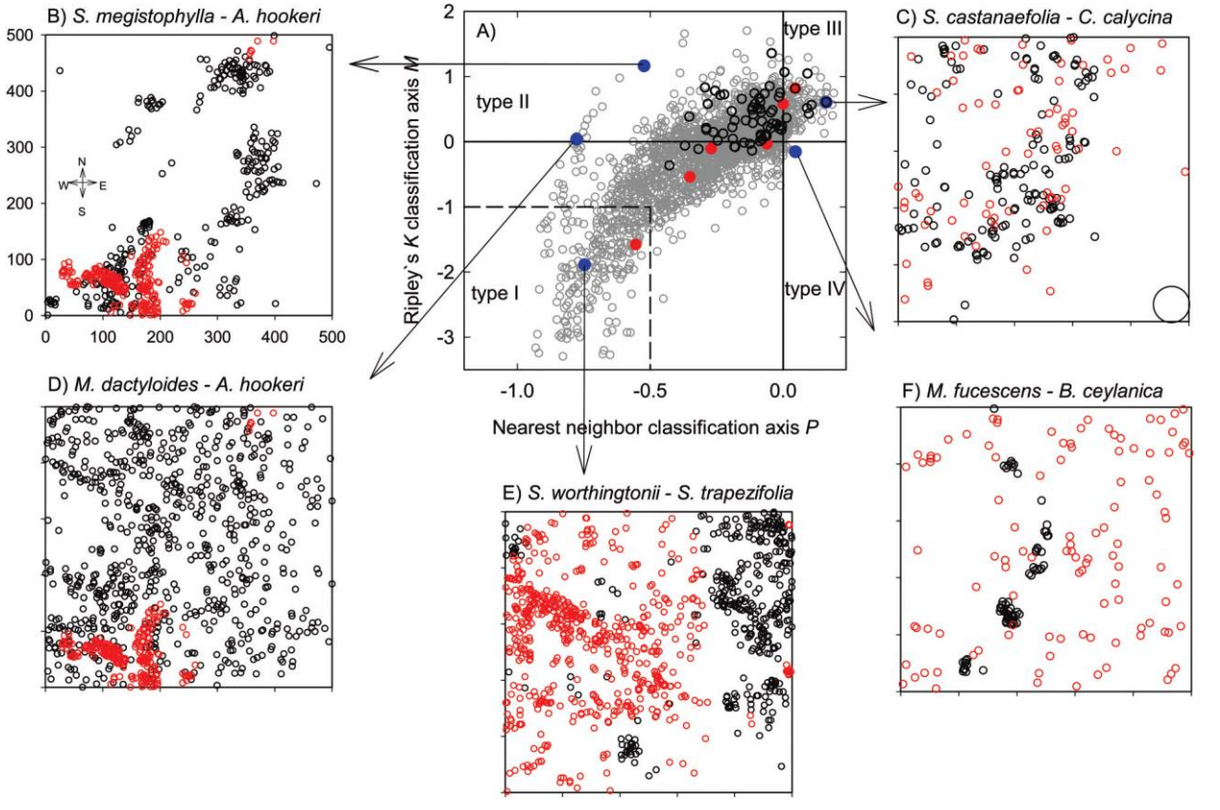

Figure 2: Classification of large-scale associations at the Sinharaja 500 × 500-m forest dynamic plot. *A*, Allocation of the large-scale association of the 2,070 species-species pairs based on the classification axes defined in equations (1). Axis *P* is positive (negative) if there are on average more (less) pattern 2 points at distance $r_L = 30$ m from pattern 1 points than expected without first- and second-order effects, and axis *M* is positive (negative) if the probability that a pattern 1 point has its nearest pattern 2 point within distance r_L is larger (smaller) than expected. The classification of individual pairs is represented as gray open circles, and black open circles mark significant and positive large-scale associations in analysis 3. The blue dots locate the four examples shown in *B*–*F*, and the red dots locate the patterns shown in figure 5. From right to left: figure 5*C*, 5*A*, 5*E*, 5*G*, 5*K*, and 5*I*. The broken line indicates the area of strong segregation. *B*, Example for type II association with partial overlap: *black circles* = species 1, *red circles* = species 2. *C*, Example for type III association with mixing and a circle with a 30-m radius. *D*, Example for a transition between type I and type II associations. *E*, Example for type I association with strong segregation. *F*, Example for a type IV association that is possible only because of a strong second-order effect of pattern 1. See text for full species names.

geneous Poisson process), the assumption of separation of scales may not hold.

Analysis 2: Bivariate Small-Scale Plant-Plant Interactions

We performed a total of 46 × 45 = 2,070 bivariate point pattern analysis for all pairs of the $n = 46$ species. The GOF test detected significant associations for 122 species pairs (=5.8%); in 54 cases, the small-scale association was positive (attraction), and in 68 cases, the small-scale association was negative (repulsion). To obtain a rough estimate of the magnitude of scale-dependent effects at different scales, we counted for each scale r the number of species (using only species where the rank of the GOF test was >95) for which the pair-correlation function was above or below the fifth-highest and fifth-lowest value of the pair-correlation function of the 99 simulations. Repulsion occurred somewhat more frequently than attraction, and pair frequencies peaked at the 2-m scale with 32 and 17 pairs, respectively (fig. 4*B*). Interestingly, significant effects were rare at scales $r > 20$ m (fig. 4*B*). These figures again outline the low occurrence of significant second-order effects in this tropical forest.

Several types of significant small-scale associations occurred at the Sinharaja FDP (fig. 5). For example, the species pair *Shorea trapezifolia–Mastixia tetrandra* showed large-scale mixing together with small-scale attraction at 0–6 m (fig. 5*C*, 5*D*). As expected, this species pair is located within the domain of association (type III; fig. 2*A*). The species pair *Semecarpus gardneri–Vitex altissima* showed

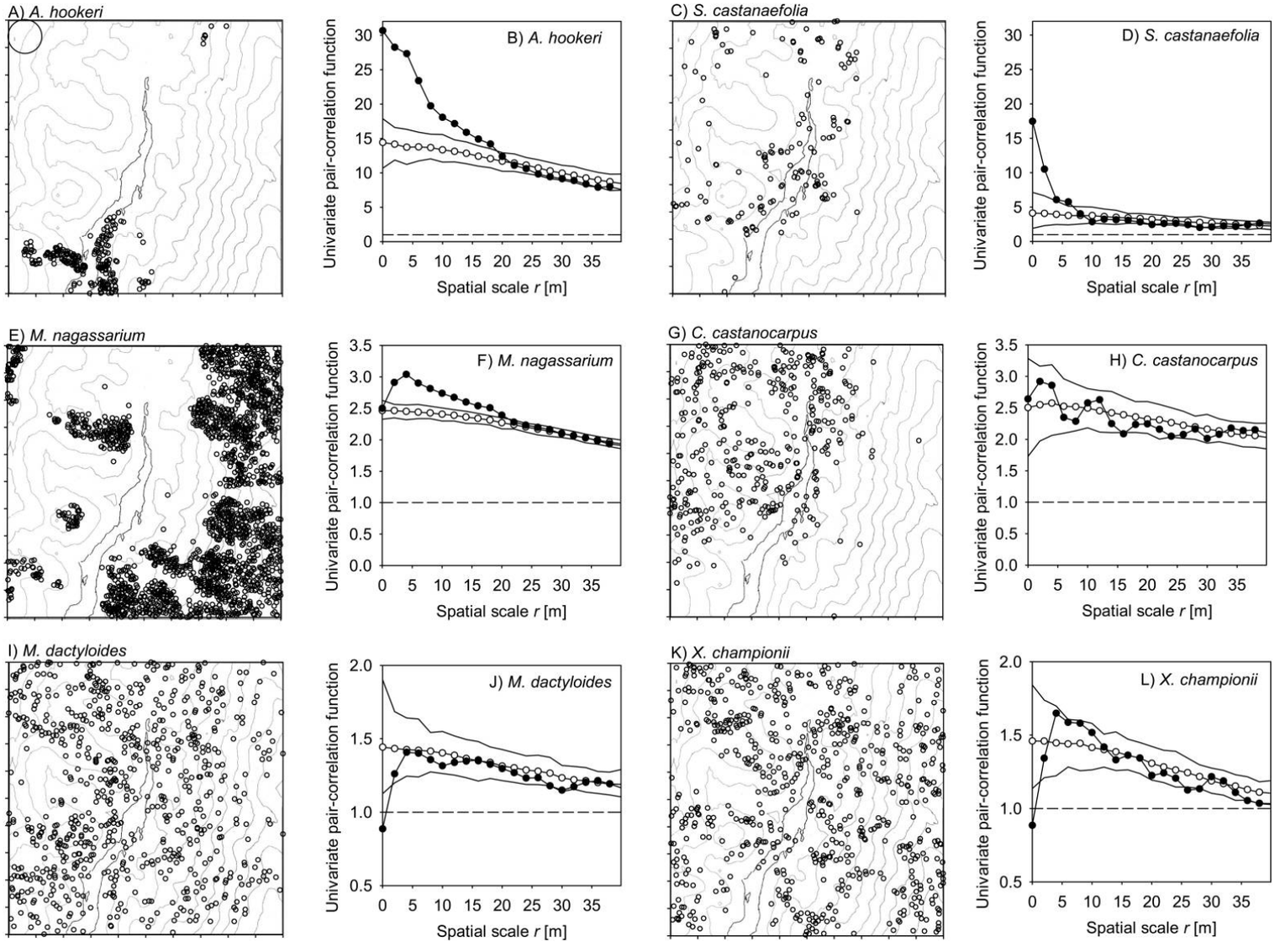
A) A. hookeri
B) A. hookeri
C) S. castanaefolia
D) S. castanaefolia
E) M. nagassarium
F) M. nagassarium
G) C. castanocarpus
H) C. castanocarpus
I) M. dactyloides
J) M. dactyloides
K) X. championii
L) X. championii
Univariate pair-correlation function
Spatial scale r [m]

large-scale mixing but significant small-scale repulsion at 0–6 m (fig. 5*A*, 5*B*). The two patterns were both located within the northwest corner of the study plot, but they formed separate clusters on smaller scales (fig. 5*A*). As a consequence of this repulsion, the species pair is located in our scheme just between mixing (type III) and partial overlap (type II; fig. 2*A*).

The next two types of association included cases where both species did not show large-scale effects in the pair-correlation function (and the K function) but did show significant small-scale repulsion or attraction. However, these types were rare. We found only one significant example (*X. championii–Cullenia ceylanica*) for small-scale repulsion where the pair-correlation function approximated a value of one for larger scales (fig. 5*E*, 5*F*). As expected, this species pair was located in our scheme close to the origin $M = 0$ and $P = 0$ (fig. 2*A*). The only example we found for small-scale attraction and large-scale neutrality (fig. 5*G*, 5*H*) showed weak segregation that shifted this pair in our scheme into the domain of segregation (type I; fig. 2*A*).

Finally, the two species may show large-scale segregation but significant small-scale repulsion or attraction. This case is exemplified by the species pair *S. trapezifolia–M. nagassarium*, which showed segregation together with repulsion (fig. 5*I*, 5*J*) and is located well within the domain of strong segregation (type I; fig. 2*A*). The species pair *Carallia calycina–Shorea affinis* showed segregation, but when trees of both species where close to each other, they showed attraction (fig. 5*K*, 5*L*). Because of their large-scale segregation, this pair is also located within the domain of segregation (type I; fig. 2*A*).

To find out whether the significance of our results was dependent on the number of stems of the species pair or on the univariate spatial structure of the component patterns, we calculated for all 2,070 species pairs the Spearman rank correlation between the rank u_0 and the number n_1 of stems of species 1, the number n_2 of stems of species 2, and the value of the pair-correlation function at scales $r = 0, 2, 6, 10, 20$, and 40 m. The rank u_0 correlated weakly and positively with the number of stems of species 2 ($r_{Sp} = 0.16$; $p < .01$) and with the number of stems of species 1 ($r_{Sp} = 0.05$, $p < .05$). Thus, the significant effects detected did not primarily depend on the sample size, although as expected, significant effects tended to be more frequent for larger sample sizes. This result also suggests that ignoring species with low abundance should not severely bias our results. We also found a negative correlation of the rank of u_0 with the pair-correlation function of species 1 at scales 0–40 m with $r_{Sp} < -0.1$, which peaked at scale 20 m ($r_{Sp} = -0.14$; $p < .01$). This indicated that we were less likely to find significant small-scale association with species that were strongly clumped at scales of about 20 m. This is reasonable, since a strong clumping of species 1 makes it less likely that points of the second species will be in contact with points of species 1 because pattern 1 points are clustered.

From the 46 species studied, only eight (*Dillenia retusa*, *Hopea jucunda*, *Hydnocarpus octandra*, *Mallotus fucescens*, *Palaquium thwaitesii*, *Shorea stipularis*, *Urandra apicalis*, *Agrostistachys hookeri*) did not show any significant association to another species. Four of these showed a very high degree of univariate clustering (*A. hookeri*, *D. retusa*, *H. jucunda*, and *M. fucescens*), and the remaining four species did not show significant univariate effects. On the other hand, cases where a species showed significant association with more than five other species were rare. The abundant subcanopy species *M. dactyloides*, which was scattered throughout the plot (fig. 3*I*), showed the highest number of significant small-scale plant-plant interactions with other species; five were positive, and four were negative. It was followed by the abundant subcanopy species *C. ceylanica* (fig. 5*E*) and canopy species *M. nagassarium* (fig. 5*I*), which showed negative interactions with six and five other species, respectively. In the other extreme, the subcanopy species *Semecarpus walkeri* showed positive interactions to five other species.

Analysis 3: Large-Scale Species-Species Association

We now investigate how often pairs of species shared the same habitat. Analogous to analysis 2, we analyzed all 2,070 possible species pairs, but now we used a heterogeneous Poisson null model where the randomization of trees of species 2 was based on the intensity function of species 1 (determined by a kernel estimate with bandwidth $h = 50$ m). Note that this null model explicitly assumed a positive large-scale association (i.e., species 2 followed the intensity of species 1) and that the null model will be met

Figure 3: Examples for univariate patterns shown at the Sinharaja forest dynamic plot. Pair-correlation functions of the data over scale r (*solid circles*), the expected g function under the heterogeneous Poison null model (*open circles*; average of simulations of null model), and the simulation envelopes (*solid lines*) being the fifth-lowest and fifth-highest $g(r)$ values of the 99 simulations of the null model. The dashed horizontal lines give the expected g function for random patterns. The null model used an Epanečnikov kernel estimate of the intensity of the pattern with bandwidth $h = 30$ m (a circle with a 30-m radius is shown in *A*). The ring width for estimation of the pair-correlation function was 4 m, and the cell size was 2 × 2 m. The patterns are shown together with contour lines every 15 m from 430 to 565 m; the 430-m line is bolded, and north is on top.

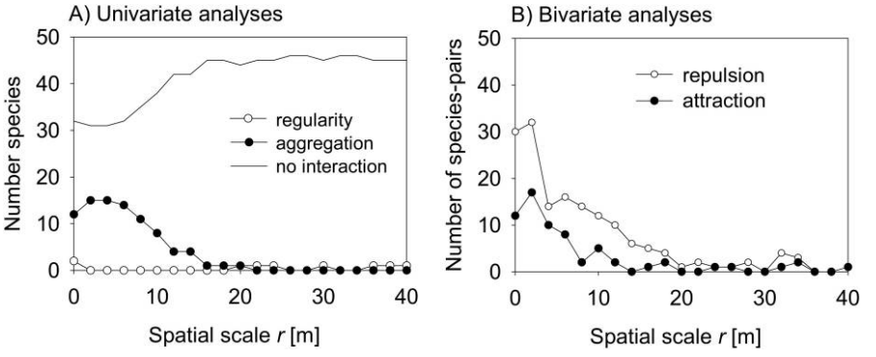

Figure 4: Number of species (univariate) and species-species pairs (bivariate) where the observed pair-correlation function is for a given scale r outside the Monte Carlo simulation envelopes, being the fifth-lowest and fifth-highest values of the simulated $g(r)$. *A*, Univariate analyses; *B*, bivariate analyses.

if the area occupied by species 2 is within the area occupied by species 1 (see appendix).

The GOF test for distance interval 50–250 m revealed significant large-scale association for 68 species pairs (3.3%). The black open circles in figure 2*A* show how these species pairs are located within our classification scheme. As expected, the associations of most of these species pairs were classified as mixing (type III) or partial overlap (type II). Only in one case (*Palaquium canaliculatus–Hopea jucunda*) was the classification axis *M* clearly negative (type I). This was because the species *H. jucunda* showed strong small-scale aggregation. An example for partial overlap is given in figure 6*A*, an example at the transition between partial overlap and mixing is given in figure 6*C*, and an example for mixing is given in figure 6*E*. When looking at small-scale effects, we found that 38 pairs showed additional small-scale repulsion, and 30 pairs showed small-scale attraction (fig. 6).

In total, 42 of the 46 species analyzed showed significant large-scale association with at least one other species. Fifteen species were in only the role of pattern 1, 13 were in only the role of pattern 2, and 14 appeared in the roles of pattern 1 and pattern 2. The species *X. championii* (fig. 3*K*) was significantly associated 11 times with a second species in the role of pattern 1, for example, with *B. ceylanica* (fig. 5*E*). The species with the next most frequent associations in the role of species 1 were *S. walkeri*, with six associations, and *M. dactyloides* (fig. 3*I*), with five associations. The species *C. calycina* (fig. 5*K*) showed, in the role of pattern 2, nine significant associations to other species, and the species *Podadeniya thwaitesii* showed five. The only species without significant large-scale association to any other species were *A. hookeri* (fig. 3*A*), *Putranjiva roxburghii*, *Shorea megistophylla*, and *Shorea stipularis*.

Discussion

We performed a comprehensive spatial pattern analysis of thousands of species-species associations at a fully mapped 25-ha forest dynamics plot of a species-rich tropical forest in Sinharaja, Sri Lanka. Our analyses were motivated by the notion that coexistence mechanisms operating in a forest should leave a spatial signature that can be detected by analyzing explicit maps of individual tree locations (Hubbell et al. 2001). In this spirit, several studies have analyzed neighborhood effects and negative density dependence in plant performance, for example, for recruitment of abundant species (Hubbell et al. 1990; Condit et al. 1992), long-term survival (Hubbell et al. 2001), mortality (Peters 2003), growth of seedlings and saplings (Connell et al. 1984; Uriarte et al. 2004), and growth of trees (Stoll and Newbery 2005). However, to our knowledge, a detailed analysis of interspecific spatial patterns has not been undertaken. One reason for this is that it would require several thousand individual point pattern analyses. An exception is a recent study by Lieberman and Lieberman (2007) on nearest-neighbor tree species combinations in tropical forests. Additionally, most patterns of individual tree species at Sinharaja, and perhaps any tropical forest (Condit et al. 2000), are heterogeneous. This causes the methodological challenge of separating first-order effects (i.e., large-scale heterogeneity, e.g., caused by environmental heterogeneity) and second-order effects (i.e., small-scale plant-plant interactions), which is necessary because first- and second-order effects interact (Wiegand and Moloney 2004) and have different biological interpretations. We faced these challenges by partitioning the general question into three complementary steps. We first categorized the types of large-scale associations caused without asking for significance and moved then to separate, more detailed

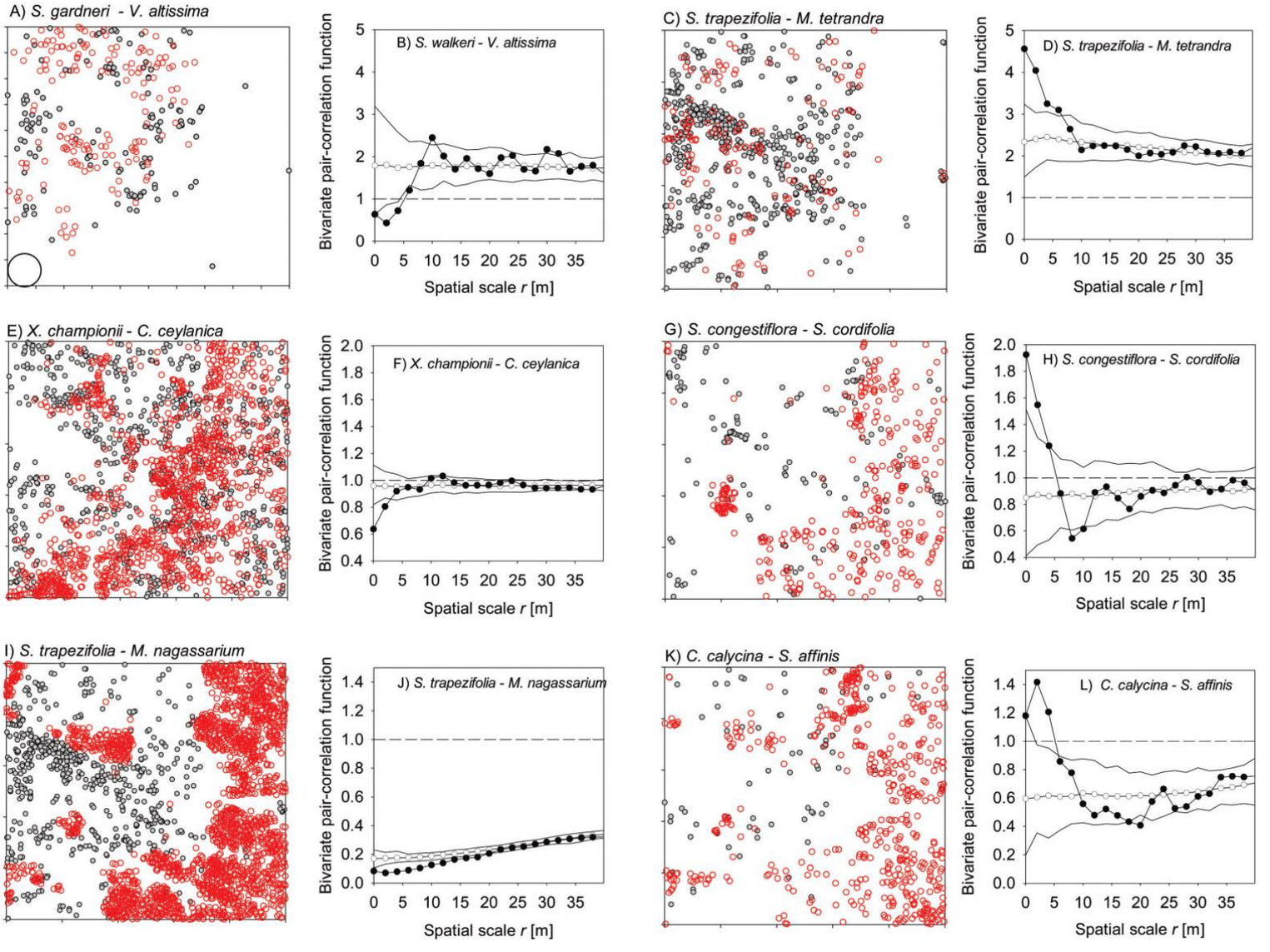
A) S. gardneri - V. altissima
B) S. walkeri - V. altissima
C) S. trapezifolia - M. tetrandra
D) S. trapezifolia - M. tetrandra
E) X. championii - C. ceylanica
F) X. championii - C. ceylanica
G) S. congestiflora - S. cordifolia
H) S. congestiflora - S. cordifolia
I) S. trapezifolia - M. nagassarium
J) S. trapezifolia - M. nagassarium
K) C. calycina - S. affinis
L) C. calycina - S. affinis
Bivariate pair-correlation function
Spatial scale r [m]

point pattern analyses to reveal significant second-order effects.

A striking result of the application of our scheme to categorize bivariate heterogeneous patterns is that only a small percentage (≈6%) of all species pairs showed an overall positive association (i.e., mixing where the area occupied by the focal pattern 1 was largely overlapped by the area occupied by pattern 2). All other species pairs showed either partial overlap (≈40%) or segregation (≈53%). This result was strengthened by our detailed point-pattern analyses, which revealed that only about 3% of all species pairs showed a significant and positive large-scale association when measured at scales >50 m (i.e., the area of species 2 was within the area occupied by species 1; note that this figure included mixing and selected cases of partial overlap). Thus, two species only rarely occupied the same areas. The common case was that some areas existed where only one of the two species was present. Interestingly, only three of the 46 species analyzed did not show any large-scale association with any other species, but only three species showed large-scale association with more than five other species. These are important results that show that the majority of the species at Sinharaja do not come close to each other.

It is well known that, simply because of the high number of species, only a few of the neighbors of an individual tree (>10 cm DBH) are likely to be conspecific, even among the most common or most highly aggregated species (Hubbell and Foster 1986; Wright 2002; Lieberman and Lieberman 2007). For example, at Sinharaja, a circular neighborhood with a 10-m radius contained on average about 25 stems with DBH >10cm. Assuming that all species were randomly distributed, this sample should contain on average about 17 different species. (For species that are homogeneously and randomly distributed through space, the number of species $S(A)$ in sampling area A is solely determined by species abundances of the community: $S(A) = S_0 - \sum_i \exp(-\lambda_i)$, where $\lambda_i = N_i/A$ is the intensity of species i and S_0 is the total number of species present in the area sampled; He and Legendre 2002.) Given the additional effect of partial overlap or segregation, it is clear that only a few species have the chance to develop specific interactions with other species and that in most cases, individuals of a given species will be associated by a different set of neighbors (Condit et al. 2002).

To verify the above hypothesis of "diffuse neighborhoods," we placed an arbitrary point inside the higher-diversity area (it had coordinates 185, 180) and determined the number of species that occurred in a circle with radius of 10 m around this point. Next we determined the number of species that occurred inside of 10-m circles but were located (on a 1-m grid) distances d away from the focal circle and determined the number of species shared with the focal circle. We found that the number of shared species declined linearly up to a distance of 20 m ($n = 75$, $r^2 = 0.74$) and then stabilized around a constant value. At distance $d = 0$, there were 17 species in the focal circle, and circles located 20–40 m away shared on average 5.3 ± 1.8 species with the focal circle. Note that the distance $d = 20$ m is the distance where the two circles do not overlap. Thus, individuals of a given species more than 20 m away from the focal individual shared in their 10-m neighborhoods on average about five out of 17 species present in the focal circle. Similar analyses with other focal points supported this result. Thus, one characteristic of species-rich tropical forest with strong habitat association and clustered individual species patterns, as found in Sinharaja, is that the set of species neighbors encountered by individuals of a given species is quite variable and not predictable for the individual. This is a sort of "spreading of risk" with respect to the neighbors. The more different species an individual may encounter in its neighborhood, the higher the chance that some individuals will have "favorable" neighbors and survive.

From this perspective, it is not surprising that only about 6% of all species-species pairs showed significant non-neutral, small-scale associations (i.e., attraction or repulsion), as revealed by our detailed point-pattern analysis of direct plant-plant interactions (analysis 2). However, considering that our goodness-of-fit test had a 5% Type I error rate, this may account for some of the apparently significant results so that the proportion of "truly" significant associations may even be lower. Interestingly, the analogous univariate analysis revealed that direct plant-plant interactions among conspecifics produced significant small-scale aggregation for about half of the species. How-

Figure 5: Examples for significant small-scale interactions. In the distribution maps, species 1 is indicated by gray and species 2 by red. The plots of the bivariate pair-correlation functions $g_{12}(r)$ over scale r show the g_{12} function of the data (*solid circles*), the expected g_{12} function under the heterogeneous Poison null model (*open circles*), and the simulation envelopes (*solid lines*) being the fifth-lowest and fifth-highest values of the Monte Carlo simulations of the null model. The dashed horizontal lines give the expected g_{12} function for independent patterns. The heterogeneous Poisson null model used an Epanečnikov kernel estimate of the intensity of the pattern of species 2 with bandwidth $h = 30$ m (a circle with a 30-m radius is shown in *A*), whereas the locations of species 1 remained fixed. The ring width for estimation of the pair-correlation function was 4 m; cell size was 2 × 2 m.

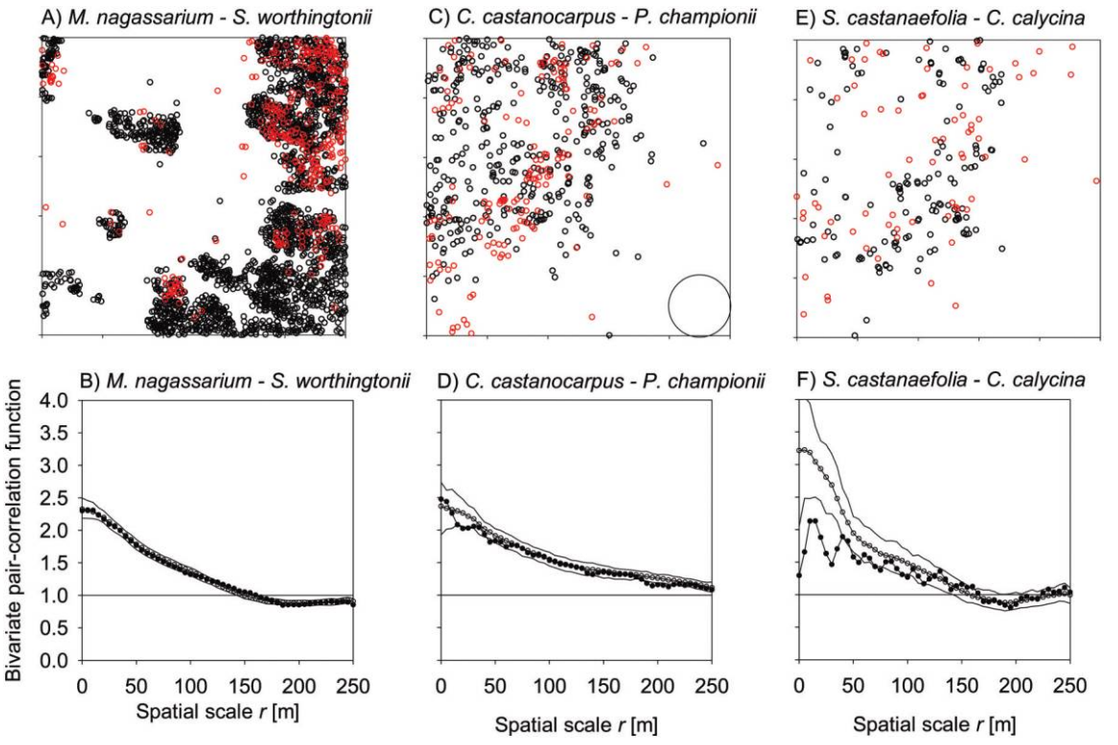

Figure 6: Examples for large-scale association. In the distribution maps, species 1 is indicated by black and species 2 by red. The heterogeneous Poisson null model used an Epanečnikov kernel estimate of the intensity of the pattern of species 1 with bandwidth $h = 50$ m (a circle with a 50-m radius is shown in *C*), whereas the locations of species 1 remained fixed. The ring width for estimation of the pair-correlation function was 10 m; grid size was 5 × 5 m. Other conventions are as in figure 5.

ever, the 6% figure is a surprisingly low figure when considering the increasing evidence for neighborhood effects on plant performance, even for larger trees. For example, Peters (2003) found that at the FDPs in Pasoh, India, and BCI, density-dependent mortality was equally common in the largest and smallest size classes. More than 80% of the species examined at each site exhibited significant or marginally significant density-dependent mortality (Peters 2003). Similarly, Stoll and Newbery (2005) found strong negative effects of conspecific neighbors on absolute basal area increment of trees between 10 and 100 cm DBH in 10 abundant dipterocarp overstory species of a lowland dipterocarp forest on Borneo. They concluded that not all neighbors were equivalent and that conspecific versus heterospecific interference effects probably played an important role in forest dynamics and community structure (Stoll and Newbery 2005).

This apparent contradiction raises the question why such non-neutral processes, which should also operate at Sinharaja, did not leave a signature in the spatial pattern. One reason could be that the studies investigating neighbor effects on tree performance and our study measured somewhat different things. Growth and mortality are dynamic processes that are measurable only using a number of snapshots (at least two) several years apart, whereas our analysis used only one snapshot. Moreover, effects of size were not included in our analysis (except that we analyzed only trees >10 cm DBH). To detect effects of size on spatial patterns, a more complex analysis would be required, for example, using the mark-correlation function (Stoyan and Stoyan 1994).

Another possibility for the contrasting results would be that the processes that shaped the patterns were non-neutral, but the patterns that finally emerged were predominantly neutral. There are two possible interpretations for this. First, non-neutral processes in tree performance may not leave a detectable spatial signature in the map of individual tree locations. The spatial pattern of mapped tree locations may therefore not be used to assess the strength of bivariate plant-plant interactions. A similar argument was recently made regarding non-neutral processes, such as niche structure, that may not leave a signature on the rank abundance curve (Purves and Pacala 2005). However, this is unlikely because spatially depen-

dent processes should create spatial structure, except in cases where for some reason the different spatially dependent processes equilibrate. This is the second interpretation. Thus, we hypothesize that a specific characteristic of species-rich tropical forests is that non-neutral processes in tree performance equilibrate and in most cases produce neutral bivariate patterns in the spatial distribution of trees. This can be interpreted as a strong argument in favor of neutral theory. The zero-sum dynamics of unified neutral theory (Hubbell 2001) captured this characteristic by simplifying the entire regeneration process from seed dispersal to adulthood (within the range of influence of large trees) into the single step of replacement where the new individual is selected with probability $1 - m$ from the local community and with probability m from the metacommunity. Thus, non-neutral processes regarding tree performance (recruitment, growth, mortality) are lumped within this step and the zero-sum dynamics assumes that there are regulating mechanisms that guarantee that the outcome of this step would be a neutral spatial pattern. This viewpoint is also supported by another result of our detailed analysis. We found that nonrandom plant-plant interactions, if present, were quite local; their range did not reach farther than about one canopy tree crown radius (<20 m). This result is in accord with other studies (e.g., Hubbell et al. 2001). Nevertheless, it would be interesting to investigate whether regeneration (i.e., trees with DBH <10 cm) shows a more pronounced signature of neighborhood effects in its spatial pattern than is shown by the larger trees studied here.

While the absence of frequent heterospecific plant-plant interactions in the bivariate spatial patterns of species pairs can be taken as support for the unified neutral theory, the strong large-scale effects, mainly segregation, do not support the assumption of the zero-sum dynamics. The large-scale effects observed at the Sinharaja plot may be attributed to a large degree to habitat association due to topography, although dispersal limitations may also contribute to this pattern. Gunatilleke et al. (2006) found in a recent analysis that of the 125 species analyzed, 99 (both abundant and less abundant) showed at least one positive or negative association to one or more of the habitats. Similar results were obtained by, for example, Harms et al. (2001) for the BCI forest dynamics plot and by Valencia et al. (2004) for a forest in Amazonian Ecuador. Valencia et al. (2004) found that topography did not provide a finely partitioned niche axis; rather, in their study it provided basically three niches. Topography thus explains some of the high local diversity in tropical forests, but the general conclusion seems to be that its overall contribution is minor (Harms et al. 2001; Svenning 2001; Wright 2002; Valencia et al. 2004). However, John et al. (2007) found in a recent study that 36%–51% of tree species at three diverse Neotropical forest plots showed strong associations with soil nutrient distributions and that the distribution of soil nutrients often correlated with topographical features such as slope and elevation. Our detailed analysis shows that large-scale habitat association may foster partial overlap or segregation between species yielding reduced probabilities of potential competitor or facilitator species to encounter each other, which may explain the low occurrence of significant second-order effects. Although the strong tendency of species to segregate may not have a primary effect, we suspect that it does have strong supplementary effects on other processes promoting species coexistence.

Acknowledgments

We gratefully acknowledge the permission given to work in Sinharaja World Heritage Site and the accommodation facilities provided by the Forest Department of Sri Lanka, as well as the generous financial assistance given to set up the plot and computerize the database by the John D. and Catherine T. MacArthur Foundation, the Smithsonian Tropical Research Institute, the National Science Foundation, and the Center for International Development at Harvard University. The manuscript benefited from comments of S. Getzin, K. Moloney, and two anonymous reviewers.

APPENDIX

Scheme to Characterize First-Order Associations of Bivariate Heterogeneous Patterns

In the first case, we assumed that pattern 1 and pattern 2 occupied only subareas A_1 and A_2 of the study area A (fig. A1*a*), and in a second case, we assumed that the two patterns occupied the entire study area but that the intensities of the two patterns followed linear gradients in the x or y direction (fig. A2).

Approximation of $K_{12}(r)$ *and* $P_0(r)$ *for Simple Cases of Heterogeneity: Subareas*

Pattern 1 and pattern 2 occurred within subareas A_1 and A_2 of the study area A, respectively, but both were random inside their respective subareas (fig. A1). Following the definition of the K function, we obtained in approximation

$$\lambda_2 K_{12}(r_L) \approx \frac{A_1 \cap A_2}{A_1}\left(\lambda_2 \frac{A}{A_2}\right)\pi r_L^2, \tag{A1}$$

where $A_1 \cap A_2$ is the overlap area between A_1 and A_2, λ_2 is the overall intensity of pattern 2 in the study plot, and πr_L^2 is the area of the circular neighborhood with radius

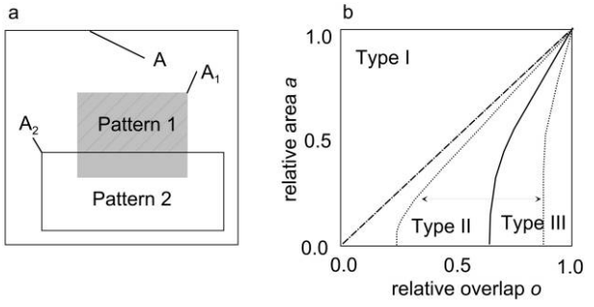

Figure A1: Classification scheme for first-order association of heterogeneous patterns. *a*, We assumed that the two patterns occupy only subareas A_1 and A_2 of study plot A that may overlap, but both patterns are random inside their respective subareas (i.e., only first-order effects—no second-order effects). *b*, Solutions of the $M = 0$ and $P = 0$ isoclines of equations (1) within the *o-a* parameter space with $M = 0$ (*dash-dotted line*) and $P = 0$ ($c = 1$: *solid line*; $c = 0.25$: *left dotted line*; $c = 2$: *right dotted line*), where c gives the expected number of pattern 2 points within circles with radius $r_L = 30$ m.

r_L. This approximation holds if the circle is smaller than the subareas (i.e., $\pi r_L^2 \ll A_i$, with $i = 1, 2$). The first factor of equations (1) follows because only pattern 1 points located inside the overlap area between A_1 and A_2 have pattern 2 neighbors and contribute to the calculation of $K_{12}(r_L)$. On the other hand, pattern 2 occurs only within subarea A_2; thus, the local density of pattern 2 is elevated relative to λ_2, yielding $\lambda_2\, A/A_2$.

With the definitions $o = (A_1 \cap A_2)/A_1$ being the degree to which pattern 1 is overlapped by pattern 2 ($0 \le o \le 1$) and $a = A_2/A$ being the relative area occupied by pattern 2 ($0 < a \le 1$), equation (A1) simplifies to

$$K_{12}(r_L) \approx \left(\frac{o}{a}\right)\pi r_L^2, \tag{A2}$$

and the expectation for the case without first-order effects (i.e., $o = 1$, $a = 1$) is

$$K_{12}^{h}(r_L) = \pi r_L^2. \tag{A3}$$

Note that the two parameters o and a in equation (A2) may scale in a way that increasing overlap o is compensated for by increasing relative area a occupied by pattern 2. Inserting equations (A2) and (A3) into equation (1) shows that the values of the axis $M = \ln(o/a)$ may range between $M = -\infty$ ($o = 0$; complete segregation) and $M = \infty$ (if both patterns occupy the same subarea [i.e., $o = 1$] but the subarea is infinitesimally small [i.e., $a = 0$]).

With arguments analogous to the derivation of equation (A1), the emptiness probability yields in approximation

$$P_0(r_L) \approx \left(1 - \frac{A_1 \cap A_2}{A_1}\right) + \frac{A_1 \cap A_2}{A_1}\exp\left(-\frac{A}{A_2}\lambda_2 \pi r_L^2\right)$$

$$= (1 - o) + o\exp\left(-\frac{c}{a}\right), \tag{A4}$$

where $c = \lambda_2 \pi r_L^2$ is the expected number of pattern 2 points in a circle with radius r_L under intensity λ_2. The first summand of equation (A4) is the proportion of pattern 1 points located outside the subarea of pattern 2 points, which always have empty circles (gray hatched area in fig. A1*a*). This summand describes the "pure" effect of segregation. The second summand is the contribution of the proportion of pattern 1 points located in the overlap area between pattern 1 and pattern 2, described by a Poisson distribution. Again, we need to consider here the locally elevated intensity of pattern 2 points ($= \lambda_2 A/A_2$). Without first-order effects, equation (A4) collapses to

$$P_0^{h}(r_L) = \exp(-c). \tag{A5}$$

The values of the axis $P = e^{-c} - (1 - o) - oe^{-c/a}$ may thus range between -1 for complete segregation and many pattern 2 points (i.e., $o = 0$ and $c \gg 1$) and e^{-c} for complete overlap (i.e., $o = 1$). In our analysis, with a minimum of 70 points, we have a minimum value of $c = 0.79$ points/circle and find $e^{-c} = 0.45$. Note that equation (A5) is an approximation that does not consider edge correction (Diggle 2003). Accordingly, we estimated the empirical distribution of nearest-neighbor distances also without edge correction.

To better understand which properties of the pattern determine the types of large-scale association (e.g., segregation, partial overlap, or mixing; fig. 2), we calculated for our approximation (eqq. [A2]–[A5]) the $M = 0$ and $P = 0$ isoclines in the *o-a* parameter space. Figure A1*b* shows that type I associations (segregation; $P < 0$, $M < 0$) arise if the relative area a occupied by pattern 2 is larger than the relative overlap o between the two patterns (i.e., $o/a < 1$). Type II (partial overlap; $P < 0$ and $M > 0$) and type I associations (mixing; $P > 0$ and $M > 0$) arise if the relative overlap o between the two patterns is larger than the relative area a occupied by pattern 2 (i.e., $o/a > 1$). Additionally, membership to type I or type II depends on the expected number of pattern 2 points in circles with radius r_L ($= c$). This is because the emptiness probability depends on the total number of pattern 2 points ($= n_2$). Under constant n_2, a type II association arises under lower relative overlap o between the two patterns and type III arises for larger relative overlap. On the other hand, for constant parameters a and o but a small number of pattern 2 points (i.e., $c \ll 1$), the emptiness probability approxi-

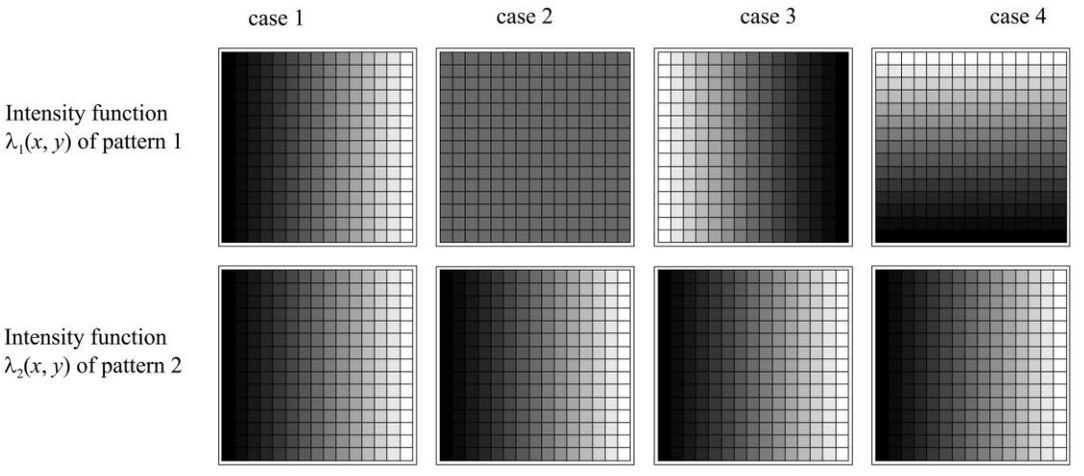

Figure A2: Different cases for the intensity functions $\lambda_1(x, y)$ and $\lambda_2(x, y)$, which follow linear gradients ($0 \pm x, y \pm d$). Black indicates zero intensity, and decreasing shading indicates higher values of the intensity functions. In case 1, patterns 1 and 2 follow the same gradient ($\alpha = 0, \beta > 0$); in case 2, pattern 1 is homogeneous ($\beta = 0$); in case 3, the two gradients are negatively correlated ($\beta = -\alpha/\mathrm{d}$); and in case 4, the gradients are oriented with an angle of 90°.

mates $P_0(r_L) \approx (1 - o) + o(1 + c/a) = 1 + c(o/a)$ and $P = P_0^h(r_L) - P_0(r_L)$ becomes 0 for $o = a$. Thus, in the extreme case where $c \to 0$, the P and the M isoclines are the same (fig. A1*b*), and only type III and type I associations occur. However, for increasing n_2, the transition type II appears. Note that a type IV association ($P > 0$ and $M < 0$) does not occur under the assumptions of our approximation, and it may arise only under strong second-order effects.

Approximation of $K_{12}(r)$ *and* $P_0(r)$ *for Simple Cases of Heterogeneity: Gradients*

In this case, we assumed that the two patterns show no second-order effects but follow linear gradients (fig. A2):

$$\begin{aligned} \lambda_1(x, y) &= \alpha + \beta x \quad \text{(cases 1, 2, and 3)}, \\ \lambda_1(x, y) &= \alpha + \beta y \quad \text{(case 4)}, \\ \lambda_2(x, y) &= \gamma x, \end{aligned} \tag{A6}$$

where the parameter β is the slope of the gradient of pattern 1 and the other parameters α and γ are determined by the normalization

$$\begin{aligned} \int_{x=0}^{d} \int_{y=0}^{d} \lambda_1(x, y) dx dy &= n_1, \\ \int_{x=0}^{d} \int_{y=0}^{d} \lambda_2(x, y) dx dy &= n_2, \end{aligned} \tag{A7}$$

where the coordinates x and y range between 0 and d. With the intensity functions defined in equation (A6), the number of pattern 2 points in a circle with radius r_L and location (x, y) yields $\lambda_2(x, y)\, \pi r_L^2$, and the K function can be calculated as

$$K_{12}(r) = \frac{d^2}{n_2} \frac{1}{n_1} \int_{x=0}^{d} \int_{y=0}^{d} \lambda_1(x, y)[\lambda_2(x, y) \pi r_L^2] dx dy. \tag{A8}$$

Solving equation (A8) yields

$$K_{12}(r) = \begin{cases} \frac{4}{3} \pi r_L^2 & \text{case 1} \\ \pi r_L^2 & \text{cases 2 and 4}. \\ \frac{2}{3} \pi r_L^2 & \text{case 3} \end{cases} \tag{A9}$$

The full solution for gradients in the intensity of pattern 1 with varying slope β (i.e., transitions between case 3 and

case 1) yields $K_{12}(r) = [1 + \beta d^3/(6n_1)]\pi r_L^2$. Thus, the possible range of the axis for linear gradients is rather limited and varies between $M = \ln(2/3) = -0.4$ and $M = \ln(4/3) = 0.29$.

As expected, the K function indicates a positive association for case 1, where the patterns follow the same gradient, and a negative association for case 3, where the gradients are negatively correlated. Interestingly, cases 2 and 4 leave no signature in the K function, pattern 1 points with few pattern 2 neighbors exactly balance pattern 1 points with many pattern 2 neighbors and consequently $K_{12}(r_L) = \pi r_L^2$.

As an analogue to the calculation of the K function, the emptiness probability yields

$$P_0(r) = \frac{1}{n_1}\int_{x=0}^{d}\int_{y=0}^{d}\lambda_1(x, y)[\exp(-\lambda_2(x, y)\pi r_L^2)]dxdy. \tag{A10}$$

We assumed here that the density of pattern 2 points was low enough so that the probability to find no pattern 2 point in a circle with radius r_L and location (x, y) would yield approximately $\exp(-\lambda_2(x, y)\pi r_L^2)$.

Equation (A10) can be solved for the intensity functions given in equation (A6). The P axis of our scheme (eqq. [1]) yields

$$P = P_0^h(r) - P_0(r) = \begin{cases} e^{-c} - \dfrac{1 - (2c + 1)e^{-2c}}{2c^2} & \text{case 1} \\ e^{-c} - \dfrac{1 - e^{-2c}}{2c} & \text{cases 2 and 4,} \\ e^{-c} - \dfrac{e^{-2c} + 2c - 1}{2c^2} & \text{case 3} \end{cases} \tag{A11}$$

where $c = \pi r_L^2(n_2/d^2)$ is the expected number of pattern 2 points in a circle with radius r_L^2 if the pattern 2 points would be homogeneously distributed (i.e., with intensity n_2/d^2). The full solution for intensities $\lambda_1(x, y)$ with varying slope β (i.e., transitions between case 3 and case 1; fig. A2) yields

$$P = P_0^h(r) - P_0(r) = e^{-c} - \left[-\beta\frac{d^3}{2n_1}\frac{(1 + c)e^{-2c} + (c - 1)}{2c^2} + \frac{c(1 - e^{-2c})}{2c^2}\right]. \tag{A12}$$

Note that case 1 corresponds to $\beta = 2n_1/d^3$, case 2 to $\beta = 0$, and case 3 to $\beta = -2n_1/d^3$ and that the minimal value of the P axis is about $P = -0.12$ for case 3.

The isoclines $P = 0$ and $M = 0$ are shown in figure A3 in dependence on slope β and the number of pattern 2 points (n_2). Segregation (type I) occurs if the slope β is negative (fig. A2). This is expected because, in this case, the intensity functions $\lambda_1(x, y)$ and $\lambda_2(x, y)$ are negatively correlated, and pattern 1 densities are high if pattern 2 densities are low, and vice versa. The transition between case 2 and case 1 in equation (A12) shows more complex behavior (i.e., β increases from 0 to β_{max}; fig. A3). In this case, the intensity functions $\lambda_1(x, y)$ and $\lambda_2(x, y)$ are positively correlated. If there are many pattern 2 points and a steep slope β, mixing (type III) occurs, whereas partial overlap (type II) occurs in the case of fewer pattern 2 points or with a less steep slope β. The change in membership with an increasing number of pattern 2 points ($= n_2$) can be understood as follows: if n_2 is small, pattern 1 points close to the right end of the gradient (i.e., $x = 500$) will have more pattern 2 neighbors than expected by a homogeneous distribution of pattern 2 points, and pattern 1 points close to the left end of the gradient (i.e., $x = 0$) will have fewer pattern 2 neighbors. Because pattern 1 points are also more frequent at the right end of the gradient, the classification axis P will have positive values. On the other hand, if there are many pattern 2 points and if pattern 2 points are homogeneously distributed, most pattern 1 points will have a pattern 2 neighbor (i.e., $P_0^h(r) \approx 0$), but in the heterogeneous case, a few pattern 1 points at the left end of the gradient will have no

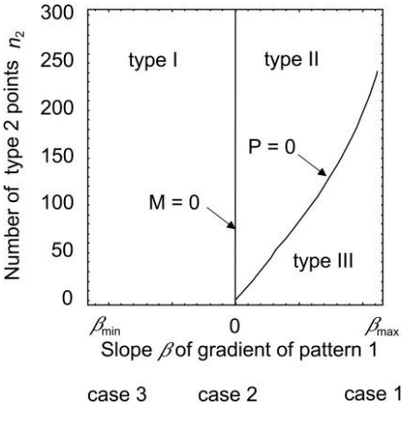

Figure A3: Solutions of the isoclines $M = 0$ (eq. [A9]) and $P = 0$ (eq. [A12]) within the $\beta - n_2$ parameter space. If the gradients in the intensity of species 1 and 2 are negatively correlated (i.e., $\beta < 0$) segregation (type I) arises. For positively correlated gradients, partial overlap (type II) or mixing (type III) may arise, depending on the number of pattern 2 points ($= n_2$). For very low values of n_2, the partial overlap type disappears.

pattern 2 neighbor. Consequently, the classification axis P will become negative.

In summary, we have shown that the potential impact of linear gradients on the location of the bivariate pattern in our scheme (fig. 2) is rather limited. In absence of strong second-order effects, the classification should therefore primarily be determined by the relative overlap between the different subareas occupied by the two patterns.

Why Is the Null Model of Analysis 3 Met If Species 2 Is Distributed Only Inside a Subarea of the Area Occupied by Species 1?

If species 2 occupies a subarea A_2 of the area A_1, which is occupied by species 1, we have $A_1 \cap A_2 = A_2$, and equation (A1) yields

$$\lambda_2 K_{12}(r_L) \approx \frac{A_1 \cap A_2}{A_1}\left(\lambda_2 \frac{A}{A_2}\right)\pi r_L^2 = \frac{A_2}{A_1}\left(\lambda_2 \frac{A}{A_2}\right)\pi r_L^2 = \left(\lambda_2 \frac{A}{A_1}\right)\pi r_L^2. \quad \text{(A13)}$$

On the other hand, the null model of analysis 3 distributes the points of species 2 following the intensity function of species 1; that is, pattern 2 points are distributed over the area A_1. In this case, we have $A_1 = A_2$ and need to replace the term $(\lambda_2 A/A_2)$ in equation (A1) with $(\lambda_2 A/A_1)$; thus

$$\lambda_2 K_{12}(r_L) \approx \frac{A_1}{A_1}\left(\lambda_2 \frac{A}{A_1}\right)\pi r_L^2 = \left(\lambda_2 \frac{A}{A_1}\right)\pi r_L^2, \quad \text{(A14)}$$

which coincides with equation (A13).

Literature Cited

Ashton, P. S. 1964. Ecological studies in the mixed dipterocarp forests of Brunei state. Oxford Forestry Memoirs 25. Clarendon, Oxford.

Baddeley, A., J. Møller, and R. Waagepetersen. 2000. Non- and semi-parametric estimation of interaction in inhomogeneous point patterns. Statistica Neerlandica 54:329–350.

Bazzaz, F. A. 1996. Plants in changing environments. Cambridge University Press, New York.

Bruno, J. F., J. J. Stachowicz, and M. D. Bertness. 2003. Inclusion of facilitation into ecological theory. Trends in Ecology & Evolution 18:119–125.

Callaway, R. M., and L. R. Walker 1997. Competition and facilitation: a synthetic approach to interactions in plant communities. Ecology 78:1958–1965.

Chave, J. 2004. Neutral theory and community ecology. Ecology Letters 7:241–253.

Chave, J., H. C. Muller-Landau, and S. A. Levin. 2002. Comparing classical community models: theoretical consequences for patterns of diversity. American Naturalist 159:1–22.

Chesson, P. 2000. General theory of competitive coexistence in spatially varying environments. Theoretical Population Biology 58: 211–237.

Clark, J. S., and J. S. McLachlan. 2003. Stability of forest biodiversity. Nature 423:635–638.

Condit, R. 1998. Tropical forest census plots. Springer, Berlin, and Landes, Georgetown, TX.

Condit, R., S. P. Hubbell, and R. B. Foster. 1992. Recruitment near conspecific adults and the maintenance of tree and shrub diversity in a Neotropical forest. American Naturalist 140:261–286.

Condit, R., P. S. Ashton, P. Baker, S. Bunyavejchewin, S. Gunatilleke, N. Gunatilleke, S. P. Hubbell, et al. 2000. Spatial patterns in the distribution of tropical tree species. Science 288:1414–1418.

Condit, R., N. Pitman, E. G. Leigh Jr., J. Chave, J. Terborgh, R. B. Foster, P. Núñez, et al. 2002. Beta diversity in tropical forest trees. Science 295:666–669.

Condit, R., P. Ashton, S. Bunyavejchewin, H. S. Dattaraja, S. Davies, S. Esufali, C. Ewango, et al. 2006. The importance of demographic niches to tree diversity. Science 313:98–101.

Connell, J. H. 1971. On the roles of natural enemies in preventing competitive exclusion in some marine animals and in rain forest trees. Pages 298–312 *in* P. J. den Boer and G. R. Gradwell, eds. Dynamics of populations. Proceedings of the Advanced Study Institute on Dynamics of Numbers in Populations, Oosterbeek, Netherlands. Pudoc, Wageningen.

———. 1978. Diversity in tropical rainforests and coral reefs. Science 199:1302–1310.

Connell, J. H., J. G. Tracey, and L. J. Webb. 1984. Compensatory recruitment, growth, and mortality as factors maintaining rain forest tree diversity. Ecological Monographs 54:141–164.

Dale, M. R. T. 1999. Spatial pattern analysis in plant ecology. Cambridge University Press, Cambridge.

Dalling, J. W., and S. P. Hubbell. 2002. Seed size, growth rate and gap microsite conditions as determinants of recruitment success for pioneer species. Journal of Ecology 90:557–568.

Dassanayake, M. D. and F. R. Fosberg. 1980–2000. A revised handbook to the flora of Ceylon. Vols. 1–12. Amarind, New Delhi.

De Rosayro, R. A. 1942. The soils and ecology of the wet evergreen forests of Ceylon. Tropical Agriculturist 98:70–80, 153–175.

Diggle, P. J. 2003. Statistical analysis of point patterns. 2nd ed. Arnold, London.

Diggle, P. J., V. Gómez-Rubio, P. E. Brown, A. G. Chetwynd, and S. Gooding. 2007. Second-order analysis of inhomogeneous spatial point processes using case-control data. Biometrics 63:550–557.

Guisan, A., and W. Thuiller. 2005. Predicting species distribution: offering more than simple habitat models. Ecology Letters 8:993–1009.

Gunatilleke, C. V. S., I. A. U. N. Gunatilleke, A. U. K. Ethugala, and S. Esufali. 2004. Ecology in Sinharaja rain forest and the forest dynamic plot in Sri Lanka's world heritage site. Wildlife Heritage Trust of Sri Lanka, Colombo.

Gunatilleke, C. V. S., I. A. U. N. Gunatilleke, S. Esufali, K. E. Harms, P. M. S. Ashton, D. F. R. P. Burslem, and P. S. Ashton. 2006. Species-habitat associations in a Sri Lankan dipterocarp forest. Journal of Tropical Ecology 22:371–384.

Harms, K. E., R. Condit, S. P. Hubbell, and R. B. Foster. 2001. Habitat associations of trees and shrubs in a 50-ha Neotropical forest plot. Journal of Ecology 89:947–959.

He, F., and P. Legendre. 2002. Species diversity patterns derived from species-area models. Ecology 83:1185–1198.

Hubbell, S. P. 1997. A unified theory of biogeography and relative species abundance and its application to tropical rain forests and coral reefs. Coral Reefs 16:S9–S21.

———. 2001. The unified neutral theory of biodiversity and biogeography. Princeton University Press, Princeton, NJ.

———. 2005. Neutral theory in community ecology and the hypothesis of functional equivalence. Functional Ecology 19:166–172.

Hubbell, S. P., and R. B. Foster. 1983. Diversity of canopy trees in Neotropical forest and implications for conservation. Pages 25–41 *in* S. Sutton, T. Whitmore, and A. Chadwick, eds. Tropical rain forest: ecology and management. Blackwell Scientific, London.

———. 1986. Biology, chance and history and the structure of tropical rain forest tree communities. Pages 314–329 *in* J. M. Diamond and T. J. Case, eds. Community ecology. Harper and Row, New York.

Hubbell, S. P., R. Condit, and R. B. Foster. 1990. Presence and absence of density dependence in a Neotropical tree community. Philosophical Transactions of the Royal Society B: Biological Sciences 330:269–281.

Hubbell, S. P., R. B. Foster, S. O'Brien, B. Wechsler, R. Condit, K. Harms, S. J. Wright, and S. Loo de Lau. 1999. Light gaps, recruitment limitation and tree diversity in a Neotropical forest. Science 283:554–557.

Hubbell, S. P., J. A. Ahumada, R. Condit, and R. B. Foster. 2001. Local neighborhood effects on long-term survival of individual trees in a Neotropical forest. Ecological Research 16:859–875.

Janzen, D. H. 1970. Herbivores and the number of tree species in tropical forests. American Naturalist 104:501–528.

John, R., J. W. Dalling, K. E. Harms, J. B. Yavitt, R. F. Stallard, M. Mirabello, S. P. Hubbell, et al. 2007. Soil nutrients influence spatial distributions of tropical tree species. Proceedings of the National Academy of Sciences of the USA 104:864–869.

Levins, R., and D. Culver. 1971. Regional coexistence of species and competition between rare species. Proceedings of the National Academy of Sciences of the USA 68:1246–1248.

Lieberman, M., and D. Lieberman. 2007. Nearest-neighbor tree species combinations in tropical forest: the role of chance, and some consequences of high diversity. Oikos 116:377– 386.

Loosmore, N. B., and E. D. Ford. 2006. Statistical inference using the *G* or *K* point pattern spatial statistics. Ecology 87:1925–1931.

Lortie, C. J., R. W. Brooker, P. Choler, Z. Kikvidze, R. Michalet, F. I. Pugnaire, and R. M. Callaway. 2004. Rethinking plant community theory. Oikos 107:433–438.

Manokaran, N., J. V. LaFrankie, K. M. Kochuman, E. S. Quah, J. E. Klahn, P. S. Ashton, and S. P. Hubbell. 1992. Stand table and distribution of species in the 50-ha research plot at Pasoh Forest Reserve. Forest Research Institute Malaysia, Kepong.

McGill, B. J. 2003. A test of the unified neutral theory of biodiversity. Nature 422:881–888.

Missa, O. 2005. The unified neutral theory of biodiversity and biogeography: alive and kicking. Bulletin of the British Ecological Society 36:12–17.

Møller, J., and R. Waagepetersen. 2003. Statistical inference and simulation for spatial point processes. Chapman & Hall/CRC, Boca Raton, FL.

Pacala, S. W., C. D. Canham, J. Saponara, J. Silander, R. Kobe, and E. Ribbens. 1996. Forest models defined by field measurements. II. Estimation, error analysis and dynamics. Ecological Monographs 66:1–43.

Peters, H. A. 2003. Neighbour-regulated mortality: the influence of positive and negative density dependence on tree populations in species-rich tropical forests. Ecology Letters 6:757–765.

Purves, D. W., and S. W. Pacala. 2005. Ecological drift in niche-structured communities: neutral pattern does not imply neutral process. Pages 106–138 *in* D. Burslem, M. A. Pinardand, and S. E. Hartley, eds. Biotic interactions in tropical forests: their role in the maintenance of species diversity. Cambridge University Press, Cambridge.

Ripley, B. D. 1976. The second-order analysis of stationary point processes. Journal of Applied Probability 13:255–266.

———. 1977. Modelling spatial patterns. Journal of the Royal Statistical Society B 39:172–212.

———. 1981. Spatial statistics. Wiley, New York.

Schurr, F. M., O. Bossdorf, S. J. Milton, and J. Schumacher. 2004. Spatial pattern formation in semi-arid shrubland: a priori predicted versus observed pattern characteristics. Plant Ecology 173: 271–282.

Stoll, P., and D. M. Newbery. 2005. Evidence of species-specific neighborhood effects in the dipterocarpaceae of a Bornean rain forest. Ecology 86:3048–3062.

Stoyan, D., and H. Stoyan. 1994. Fractals, random shapes and point fields: methods of geometrical statistics. Wiley, Chichester.

Svenning, J.-C. 2001. On the role of microenvironmental heterogeneity in the ecology and diversification of Neotropical rain-forest palms (Arecaceae). Botanical Review 67:1–53.

Tilman, D. 2004. Niche tradeoffs, neutrality, and community structure: a stochastic theory of resource competition, invasion, and community assembly. Proceedings of the National Academy of Sciences of the USA 101:10854–10861.

Uriarte, M., R. Condit, C. D. Canham, and S. P. Hubbell. 2004. A spatially explicit model of sapling growth in a tropical forest: does the identity of neighbours matter? Journal of Ecology 92:348–360.

Valencia, R., R. Foster, G. Villa, R. Condit, J. C. Svenning, C. Hernandez, K. Romoleroux, E. Losos, E. Magard, and H. Balslev. 2004. Tree species distributions and local habitat variation in the Amazon: a large plot in eastern Ecuador. Journal of Ecology 92:214–229.

Volkov, I., J. R. Banavar, F. He, S. P. Hubbell, and A. Maritan. 2005. Density dependence explains tree species abundance and diversity in tropical forests. Nature 438:658–661.

Whitmore, T. C. 1984. Tropical rain forests of the Far East. Clarendon, Oxford.

Wiegand, T., and K. A. Moloney. 2004. Rings, circles, and null-models for point pattern analysis in ecology. Oikos 104:209–229.

Wills, C., K. E. Harms, R. Condit, D. King, J. Thompson, F. He, H. C. Muller-Landau, et al. 2006. Non-random processes maintain diversity in tropical forests. Science 311:527–531.

Wong, Y. K., and T. C. Whitmore. 1970. On the influence of soil properties on species distribution in a Malayan lowland dipterocarp forest. Malayan Forester 33:42–54.

Wootton, J. T. 2005. Field parameterization and experimental test of the neutral theory of biodiversity. Nature 433:309–312.

Wright, S. J. 2002. Plant diversity in tropical forests: a review of mechanisms of species coexistence. Oecologia (Berlin) 130:1–14.

Associate Editor: Thomas N. Sherratt
Editor: Monica A. Geber